

Tectonic Processes on Europa: Tidal Stresses, Mechanical Response, and Visible Features

Richard Greenberg, Paul Geissler, Gregory Hoppa, B. Randall Tufts, and Daniel D. Durda

Lunar and Planetary Laboratory, University of Arizona, Tucson, Arizona 85721
E-mail: greenberg@lpl.arizona.edu

Robert Pappalardo and James W. Head

Department of Geological Sciences, Brown University, Providence, Rhode Island 02912

Ronald Greeley and Robert Sullivan

Department of Geology, Arizona State University, Tempe, Arizona 85287

and

Michael H. Carr

Astrogeologic Studies, U.S. Geological Survey, Menlo Park, California 94025

Received September 26, 1997; revised March 3, 1998

I. INTRODUCTION

Europa's orbital eccentricity, driven by the resonance with Io and Ganymede, results in "diurnal" tides (3.5-day period) and possibly in nonsynchronous rotation. Both diurnal variation and nonsynchronous rotation can create significant stress fields on Europa's surface, and both effects may produce cracking. Patterns and time sequences of apparent tectonic features on Europa include lineaments that correlate with both sources of stress, if we take into account nonsynchronous rotation, after initial crack formation, by amounts ranging up to several tens of degrees. For example, the crosscutting time sequence of features in the Cadmus and Minos Linea region is consistent with a combined diurnal and nonsynchronous tensile-stress field, as it evolves during tens of degrees of nonsynchronous rotation. Constraints on the rotation rate from comparing Voyager and Galileo images show that significant rotation requires $>10^4$ yr, but could be fast enough to have allowed significant rotation since the last global resurfacing, even if such resurfacing was as recent as a few million years ago. Once cracking is initiated, diurnal tides work cracks so that they open and close daily. Although the daily effect is small, over 10^5 yr double ridges could plausibly be built along the cracks with sizes and morphologies consistent with observed structures, according to a model in which underlying liquid water fills the open cracks, partially freezes, and is extruded during the daily closing of the cracks. Thus, several lines of observational and theoretical evidence can be integrated if we assume nonsynchronous rotation and the existence of a liquid water layer. © 1998 Academic Press

Key Words: Europa; geological processes; ices; tectonics; tides.

The mechanics of the visible surface of Europa, as observed recently by the imaging system of the Galileo spacecraft, and 18 years earlier by Voyager at much lower resolution, are expressed by a global network of lineaments, apparently representing cracks, over the entire icy surface. A major driver for the geology and geophysics of Europa must be tidal deformation produced by Jupiter. Tides generate periodic diurnal global stresses (Jeffreys 1961); they provide the dominant internal heat source, possibly capable of maintaining a liquid water ocean (Cassen *et al.* 1982, Squyres *et al.* 1983, Ross and Schubert 1986, Ojakangas and Stevenson 1989a); and they exert torques which may have given Europa a nonsynchronous rotation rate with corresponding large, long-period tidal stresses (Greenberg and Weidenschilling 1984). The observed tectonic structures on Europa can be interpreted by geological modeling in the context of understanding of tidal processes.

In this paper, we review the mechanisms of tidal deformation (Section II), including "diurnal" strain due to orbital eccentricity, the consequent possible nonsynchronous rotation, and the additional strain that would follow from such rotation. We show in Section III how diurnal effects might plausibly build up the ridges that appear to line both sides of crustal cracks, and in Section IV we show how that process can explain the character and appearance of the ridges. In Section V, we compute the tidal strain pat-

terns to be expected from nonsynchronous rotation and from diurnal tides and review the correlation of these patterns with the locations and orientations of cracks.

Together, these considerations provide a model in which currently observed cracks were produced as Europa rotated through the last several tens of degrees relative to the direction of Jupiter, with crack patterns affected by stress due to both nonsynchronous rotation and diurnal tides, possibly during the past several hundred thousand years. According to this model, evolution of such lineaments due to periodic working by diurnal tides continued after the initial cracking, so that we now observe features representing a range of ages, characterized by the orientations that reflect the global stress at the time of initial cracking and by the degree of subsequent maturity of ridge structures. The model is based on the notions of a liquid-water layer below a thin lithosphere (supported by various geological evidence, e.g., Carr *et al.* 1998), a relatively youthful surface (supported by crater statistics, e.g., Chapman *et al.* 1997), and a nonsynchronous rotation rate.

II. COMPONENTS OF TIDAL DEFORMATION

If Europa's orbit were circular, its tidal evolution would not have been interesting. Tidal torque would have rapidly spun the satellite (in $\sim 10^5$ yr) until it rotated synchronously with its orbital period (about 3.5 days), after which the tidal bulge would be fixed relative to the body of the satellite (Peale 1977). In that simple history, while significant stress would develop during the spin-down (Helfenstein and Parmentier 1983), the short duration of that process suggests it would have been so early that impact cratering would have erased any record of tectonic effects.

Until quite recently, Europa's rotation was widely believed to be synchronous. In part, this belief was based on tabulations of the orbital eccentricity e as zero (e.g., it appears as 0.000 in Morrison *et al.* 1977). This misleading value propagated from a tradition in celestial mechanics of recording only the free component of e , which does not include gravitationally forced components. The rationale for such tabulations was that mathematically the free component is analogous to the parameter e in the two-body problem, because it is a free parameter defined by initial conditions. However, the actual e for Europa is dominated by a component forced by the gravitational resonance with Io and Ganymede, with a value $e = 0.01$. It was not until Peale *et al.* (1979) combined geophysical calculations with parameters for the actual motion of the Galilean satellites that the correct values of e became widely known, along with their implications for on-going tidal heating.

For a satellite on an eccentric orbit, even if it rotates synchronously, the magnitude and orientation of the tidal distortion due to the planet changes with a period equal to the orbital period. The tide-raising gravitational poten-

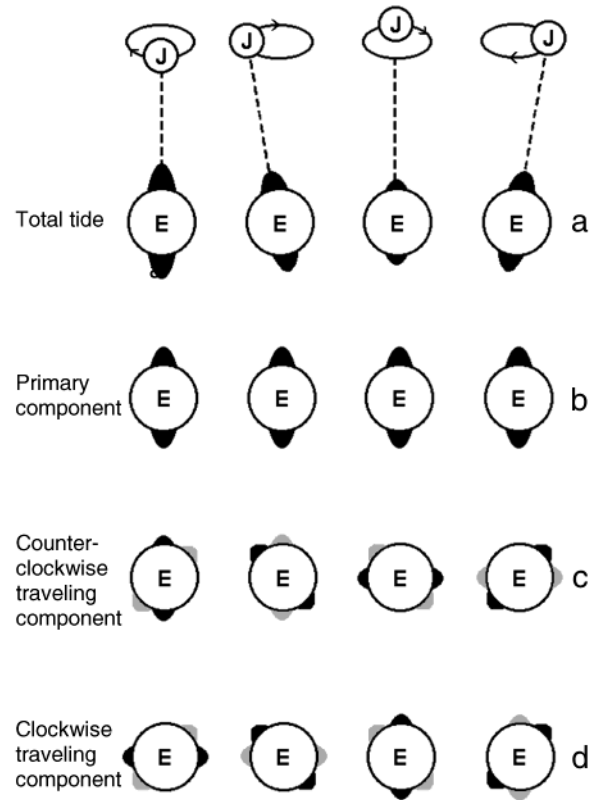


FIG. 1. Schematic representation of "diurnal" variation of tides raised on Europa by Jupiter: (a) shows the epicyclic motion of Jupiter over one orbital period (in four steps, starting with pericenter at left) viewed in a reference frame rotating at the average orbital angular velocity. The tidal amplitude is greatest at pericenter, etc. (b) shows the primary tidal component, which is of constant magnitude, aligned with the mean direction of Jupiter. If Europa rotates synchronously, the primary component produces no tidal stress on the body; if Europa rotates nonsynchronously, the primary component can potentially produce substantial stress. The variability of the tide over an orbit can be described by two Fourier components, traveling waves moving counterclockwise (c) and clockwise (d). Due to dissipation, these traveling components may lag slightly in phase from the nominal orientations shown here. Such a lag can be represented mathematically by addition of very small components 45° behind each wave as shown by the gray bulges.

tial is at a maximum at pericenter and a minimum at apocenter. Moreover, the orientation of the tide advances ahead relative to the body of the satellite after pericenter and falls behind before pericenter (Fig. 1). We refer to this periodic change as the "diurnal" variation, because it corresponds to a day on Europa (which is nearly identical to Europa's orbital period) and at 85 hr it is also comparable to the original, Earth-centric, definition of the diurnal period.

The tide can be broken into several Fourier components (Jeffreys 1961). The first is the primary component, which is independent of e . This component moves around at the same rate as synchronous rotation, thus not distorting the

satellite assuming that the body's rotation is in fact synchronous with the orbital period. The amplitude of the primary component is ~ 500 m, proportional to the mass of Jupiter and inversely proportional to a^3 (a is the mean distance to Jupiter).

Another component of the tide is a standing wave that alternately raises bulges (a) aligned with the sub-Jupiter and anti-Jupiter points with maximum height at pericenter and (b) aligned with the leading and trailing faces with maximum height at apocenter. This standing wave adds to the amplitude of the primary component at pericenter and subtracts from the amplitude at apocenter; it accounts for the variation of the amplitude of the total tidal bulge with the periodically varying distance from Jupiter. The standing wave (the "amplitude-varying standing wave") is composed of two waves traveling around Europa in opposite directions.

Another important component of the variable tide is a standing wave that alternately raises small bulges aligned 45° ahead of the orientation of the primary component (peaking $1/4$ orbital period after pericenter) and 45° behind the orientation of the primary component (peaking $1/4$ orbital period after apocenter). This standing wave, when added to the primary component, alternately shifts the direction of the total tide slightly ahead and slightly behind the mean direction of Jupiter; it accounts for the variation in the direction of Jupiter due to Europa's periodically changing velocity on its eccentric orbit. This standing wave (the "direction-varying standing wave") is also composed of two waves traveling around Europa in opposite directions.

In fact, the two traveling waves that compose the direction-varying standing wave are the same two traveling waves that compose the amplitude-varying standing wave, except for different coefficients. Thus, the major components of diurnal tides are equivalent to the two traveling waves represented in the bottom two rows of Fig. 1. Note that each wave moves around Europa relative to the direction of Jupiter at a rate such that the wave peaks move halfway around in each orbital period. The wave that moves in the prograde direction has an amplitude of $(14/3)e$ times the amplitude of the primary (nondiurnal) component. The wave that moves in the retrograde direction has an amplitude of $-(2/3)e$ times the amplitude of the primary (nondiurnal) component. (The minus sign reflects the opposite phase as shown in Fig. 1.)

The traveling waves shown in Fig. 1 represent the orientations for idealized instantaneous response to Jupiter's tide-raising potential. In fact, because the real material that composes Europa cannot respond instantaneously, the traveling waves' components must lag behind the positions shown. One can account for this lag by adding a very small wave traveling 45° behind each of the wave components, as shown by the gray bulges in Fig. 1. Note that the lag

components are oriented 45° from the direction of Jupiter at pericenter, so there can be significant time-averaged tidal torque even for synchronous rotation. In this paper, we describe the significant implications if this torque causes rotation to be slightly nonsynchronous.

Even if the tidal torque is insufficient to break the lock to synchronous rotation, the diurnal variations cause continual short-period flexing of Europa. The amplitudes of this distortion are smaller (by a factor $\sim 7e$) than the primary component, but the frequency is so great that it is worth considering whether the cumulative effect is great enough to have significant geological effects. In the next section, we consider the effects of diurnal working on pre-existing cracks and show that they may be significant and even dominant in governing the formation of ridges. In Section IV we discuss how consistent are the characteristics and morphologies of these structures with formation by this proposed process. In Section V we show how diurnal tidal stress, as well as the tidal stress of nonsynchronous rotation caused by diurnal dissipation, may have played a major role in initial creation of cracks and in governing their global patterns.

III. EFFECTS OF THE DIURNAL TIDES ON PREEXISTING CRACKS

In order to quantify the possible effect of diurnal tides on preexisting cracks, we consider a plausible mechanism that has been proposed to explain the formation of the long linear ridges discovered on Europa by Voyager (Lucchita and Soderblom 1982) and imaged at much higher resolution by Galileo (Belton *et al.* 1996, Greeley *et al.* 1998). The model, by Pappalardo and Coon (1996), is based on studies of ridge formation on Arctic sea ice.

The analogy may be appropriate for Europa. Evidence that Europa's ice shell is mobile was reported by Schenk and McKinnon (1989). Moreover, as reviewed by Carr *et al.* (1998), Europa's crust may consist of ice only a few kilometers thick overlaying liquid water. The strongest evidence for this structure comes from images of regions of the surface where blocks of crustal ice seem to have floated and drifted over a liquid sea. The height of these blocks above the surface in which they appear to have floated is ~ 100 m, suggesting block thickness of only one or two kilometers. That value would also be the thickness of the global ice crust if these floating blocks are representative. In the context of the model developed here, the crust is defined as the entire solid layer down to liquid water. (Note that evidence regarding the crustal thickness based on the observation that topography seems to be limited to heights of about 200 m, or on interpretation of downwarping adjacent to ridges, does not constrain the thickness of a lower portion of the crust that is probably a viscous solid on long time scales.)

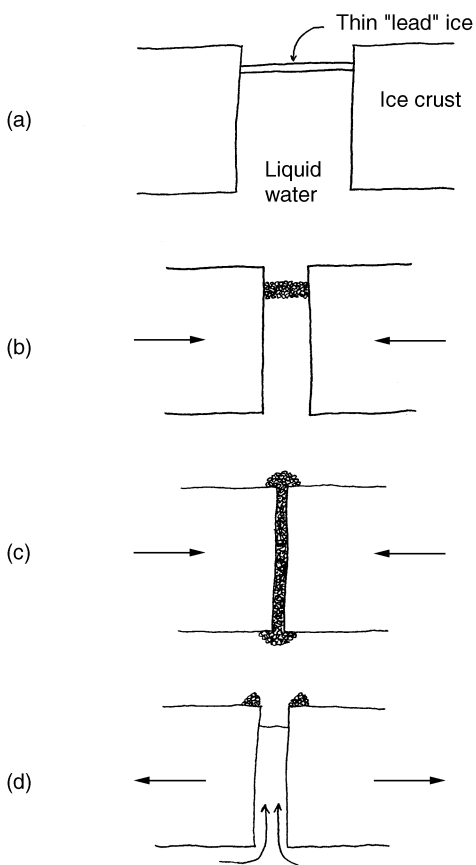


FIG. 2. A model for ridge formation by diurnal working of a preexisting crack. (a) After the crack opens and fills with liquid water, ice quickly forms at the fresh surface. (b) The crack then closes, forming a narrowing, but vertically thickening, raft of crushed ice. (c) Some of the slurry is squeezed onto the surface as the crack closes. (d) The crack reopens, leaving a double ridge of surface deposit, and liquid water enters renewing the cycle.

Some theoretical calculations of tidal heating also support the possibility of a substantial global ocean. As discussed above (Section I) the diurnal tide may dissipate enough energy to maintain an ocean. Moreover, that calculation depends on the preexistence of an ocean. If liquid water were not thickly and globally distributed, the rigidity of Europa would reduce the tidal amplitude and the tidal heating, such that liquid water could not be maintained. This line of argument suggests that any evidence for liquid water may also be evidence for a global ocean.

The model by Pappalardo and Coon was proposed before the Galileo imaging of Europa and assumed more substantial local strain and longer time scales than given by diurnal tides. Nevertheless, we can quantify the effect of diurnal tides on such a model. The process (illustrated in simple form in Fig. 2) occurs as follows. (a) An existing crack in the ice crust opens, and liquid water from below

fills the gap to the float line (about 10% of the way down from the surface). Thin ice forms at the new surface (called "lead ice" in Arctic studies). Within a few hours, the lead ice freezes to about 0.5 m in thickness (Reynolds *et al.* 1983). The freezing process would be very dynamic, accompanied by boiling in the near vacuum, so the lead ice might be very weak, porous, and irregular. (b) As global stress reverses, the crack begins to close. Lead ice is fragmented in the process. The raft of buoyant crushed ice becomes thicker inversely with the closing of the crack width, which is further enhanced by continued freezing of newly exposed water. (c) As the crack approaches closure, it is so thin that the top of the now-thick raft of crushed ice (perhaps as a slurry with boiling interstitial liquid) is squeezed onto the surface, building a ridge. Simultaneously, even more material would be squeezed down below the ice, but for the moment we assume that it remelts quickly in the relatively warm water. (d) In the next diurnal cycle, the crack reopens, with some debris falling back into the crack, leaving ice debris in ridges at the surface along both sides of the crack, as the process begins to repeat itself.

We can quantify this model using the known scale of the diurnal tides. (A detailed discussion of the distribution of surface strain is included in Section V.B below). The amplitude of the diurnal tide is 15 m (30 m from minimum to maximum). Thus, the diurnal tide introduces surface strain, required to accommodate the tidal distortion, of about 1 m per 100 km across the surface. This strain will open and close cracks. Linear ridge structures are densely packed on most regions of Europa that have been imaged at high resolution, but their superposition suggests they represent a range of ages, with freshest ridges tens of kilometers apart. If we assume the spacing between active cracks at any one time is typically ~ 100 km, the open cracks would be about a meter wide. Given the thickness of expected lead ice, it follows that the cross section of crushed ice produced in each crack in each diurnal cycle would be about 0.5 m^2 (i.e., about 0.5 m^3 per linear meter along the crack) per 85-hr day. If about 10% of this material is squeezed out onto the surface (most is squeezed back down into the subcrustal ocean), enough volume would be cumulatively deposited on both sides of the crack to make ridges 1 km wide and 100 m high in only about 30,000 yr. This calculation shows that the small scale of diurnal tides is effectively compensated by their high frequency, so that ridge structures can be built very fast.

As described in the next section, actual ridges observed on Europa are of the size considered above. Many are substantially smaller, requiring correspondingly shorter formation times. Others are larger and more complex, with several times greater volume, suggesting more extensive accumulation of extruded material. However, the longer times of accumulation required even for such large ridges are within the youngest surface age (\approx a million years)

suggested as consistent with crater statistics (Chapman *et al.* 1997), with a very wide margin.

The efficiency of extrusion calculated above could be affected by a number of factors. The irregular walls of a real crack might prevent the idealized quantity of crushed ice from reaching the surface. On the other hand, bumpy walls (as well as any crushed ice that failed to be extruded either up or down below the crust in previous cycles) might contribute additional material to the raft of crushed ice, especially if the diurnal variation of stress includes a periodic shearing phase as well as simple opening and closing. Moreover, the continual freezing of additional exposed water during the 40 hr that the ice is crushed by the closing crack could enhance the production of material for extrusion.

The ridge formation rate that we have estimated is so rapid that even if the efficiency of extrusion of crushed ice is a factor of 50 less, the ridges observed on Europa could still have been produced in less than the shortest estimates (a few million years from crater statistics) of the age of the current surface. This result demonstrates that diurnal tides, although small, are frequent enough to have played a significant role in European geology. In the following sections, we describe several classes of tectonic structures observed on Europa and then show how their character may be explained by our model of the effects of diurnal tides on preexisting cracks.

IV. CHARACTERISTICS OF LINEAR RIDGES

The most numerous linear, and presumably tectonic, features on Europa are simple pairs of ridges, the largest on the order of 100 m high and a kilometer wide with a gap between them of comparable width (Fig. 3). Higher resolution images show similar structures of lesser height and width. These features are distributed everywhere we have images of adequate resolution and are presumably ubiquitous globally.

A second class of linear feature has much wider ridges on both sides of the central valley. These ridges are lineated along their length, such that in most cases they appear to comprise multiple subridges, and these structures are generally symmetrical in cross section about the central valley (Fig. 4). Although the ridges are considerably wider than the simple pairs, the elevation is typically limited to less than 200 m.

Finally, a third class, often associated with large-scale global lineaments consists of braided, intertwined, mutually crossing ridge complexes. Some components of these complexes appear to be simple pairs; some components are wider, like class 2. An excellent example is Agave Linea (Fig. 5). While class 2 features appear in plan view as two-lane roads, class 3 features are complex systems of multilane highways with multiple service roads and on- and off-ramps.

Independent of class, ridges cross cut one another, as if generation after generation has been formed. Their plan views are quite variable, including very straight, curvilinear, and sinuous. The cycloidal, arcuate ridges on Europa have been found to be of class 1 in the few cases where adequate resolution is available to distinguish their structure.

Ridges of the second and third class are often bordered by diffuse regions of darker surface material, forming what were identified in the lower resolution Voyager and Galileo (orbit G1) images as "triple bands." Wherever multispectral data are available, this dark border is relatively red. At the higher resolutions obtained by Galileo imaging, the dark border regions seem to be characterized by subdued texture with their extent limited by confining topography. Ridges of class 3, and to some extent class 2 as well, are also often accompanied by parallel sets of linear cracks on both sides of the ridge complex, in some cases extending quite far out on both sides.

All of the characteristics of these classes of ridges can be interpreted as consequences of the ridge formation model discussed in Section III. The simple ridge pairs (class 1) are the expected result of the diurnal tidal process as described there (see Fig. 6a). The fact that the amount of ridge material extruded is limited, and that there are multiple cross-cutting generations of ridge pairs, suggests that these cracks are active for durations much shorter (probably a few million years) than the age of the surface. The complicated, and evidently changing orientations of these features may indicate that the diurnal strain patterns gradually change, perhaps due to global reorientation as Europa slowly rotates, nonsynchronously, relative to Jupiter (as discussed in later sections below).

The wider, symmetrical ridges (class 2) may simply represent much more mature versions of class 1, in which a longer duration of diurnal pumping has extruded more material, which has spread laterally and symmetrically due to the symmetrical nature of the process. In cases where the width is more extreme, other effects may be playing a role. As described in Section III, extrusion of crushed ice may not always be completely efficient; some fraction of the crushed ice may remain jammed between the walls. In that case, with each diurnal closure, the original walls (and the original extruded ridges) of the crack may be ratcheted gradually apart. Additional extrusion of crushed ice slurry will be between the original ridges, gradually producing the symmetrical ridge sets with the crack at their center (Fig. 6b), similar to the symmetrical emplacement of volcanic material around terrestrial sea-floor spreading centers.

As the quantity of material deposited adjacent to cracks increases, it presses down on the crustal ice that supports it, causing downwarping of the crustal plate (Pappalardo and Coon 1996). The weight of the ridge may be isostatically compensated to some degree if the diurnal extrusion

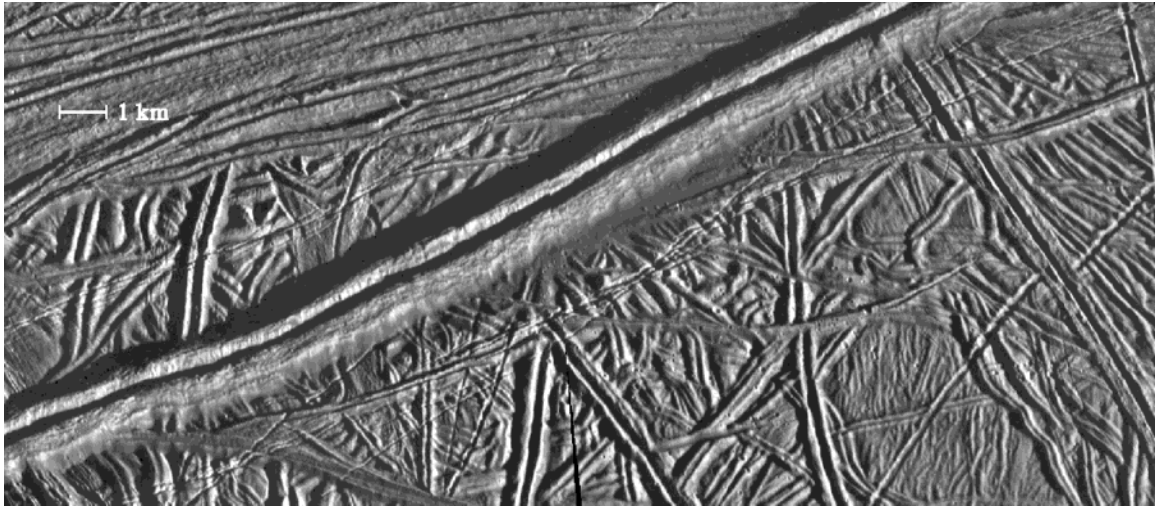


FIG. 3. Examples of Class 1 lineaments in the Bright Plains region imaged by Galileo on orbit E6. The prominent ridge pair running from lower left to upper right is an example of a larger Class 1 feature, which might form as quickly as 30,000 yr according to the calculations in this paper. (The possibly flooded margins suggest that this feature may have been massive enough to promote crustal downwarping and consequent flooding; the central groove shows evidence of fall-back of debris as the crack was worked by diurnal tides.) Numerous smaller examples of Class 1 pairs are also evident in this region, and may have formed even more quickly, or may have been active when there was less diurnal working. Running from the lower right perpendicular to the prominent ridge pair is an example of a small Class 2 structure, with multiple ridges (two on each side in this case), symmetrical about the central groove.

creates a significant keel of ice to be extruded downward under the crack region. However, such compensation would be minimal if the keel melts in the warm water as we assumed above (see also Tufts 1993). Even if the keel becomes substantial, it is likely not to be distributed identically to the ridge above it, so down-tilting torques are still probable (Coon 1997, private communication, Parmerter and Coon 1972).

Downwarping of crust under the load of the ridges could

cause lateral cracking, running parallel to the ridges. This effect was sketched by Pappalardo and Coon (1996) and is similarly illustrated in Figs. 6b and 6c, although the numbers, density, and extent of such cracks seen on Galileo images (e.g., in Fig. 4) is actually much greater. Once these lateral cracks form, it is possible that some of them become a new or alternate site for diurnal expansion and contraction. Ridges of class 1 may begin to grow around these cracks. In fact, as time goes on, different cracks may be

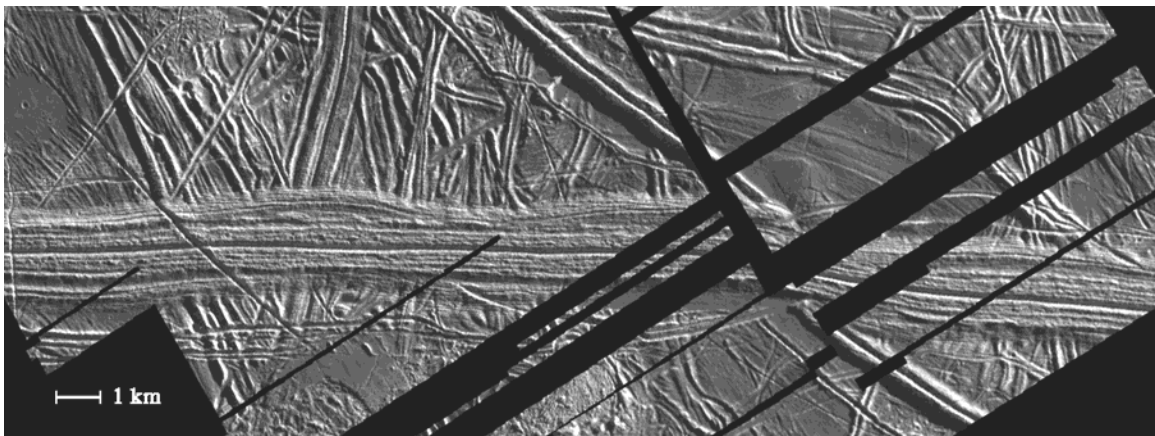


FIG. 4. An example of a large, mature Class 2 structure. The kilometer-wide central band includes multiple lineaments symmetrical about the central groove, characteristic of Class 2. This lineament represents a spreading center, as evidenced by the alignment of features on the surrounding terrain upon reconstruction, which is consistent with our model of formation of Class 2 ridges as cracks ratcheted open during diurnal working. The lineament appears to have generated parallel side cracks, associated with crustal downwarping in our model, and some appear to have developed ridge structures, so that this lineament has begun to evolve into Class 3.

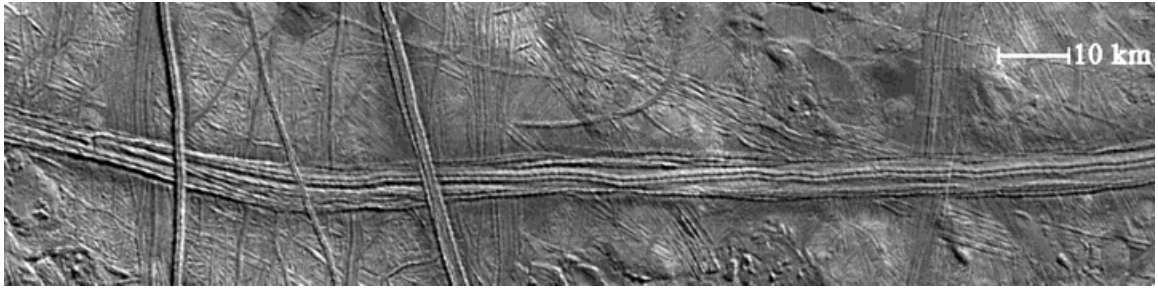


FIG. 5. Agave Linea is an example of a mature Class 3 structure. Interbraided pairs of ridges may represent activated side cracks that, in addition to the original central crack, have been worked by diurnal tides. Several examples of apparently older, subdued Class 3 structures are crossed by Agave Linea and can be seen in this mosaic of E6 images adjacent to the Conamara Chaos region. The prominent Class 1 ridge pair seen at the right, running perpendicular to Agave Linea, is the same feature that appears prominently in Fig. 3.

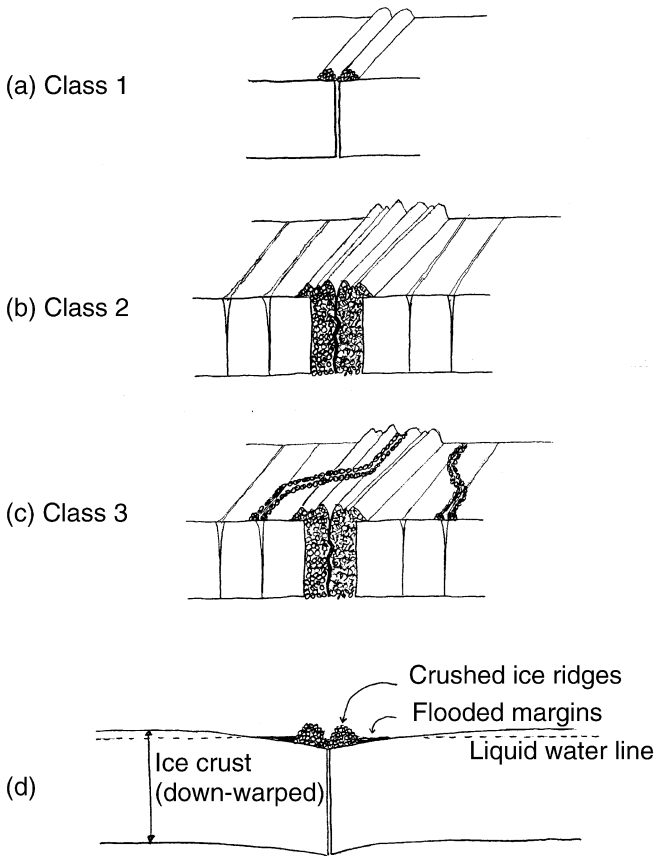


FIG. 6. Schematic cross-sections of the classes of ridges defined here, showing structure expected on the basis of our model of their formation. (a) Class 1 forms by repetitive diurnal working as shown in Fig. 2. (b) Incomplete extrusion of ice debris allows a crack to ratchet open during the diurnal working, creating a Class 2 ridge structure. If there is crustal downwarping due to the load, parallel side cracks may form. (c) Diurnal working may activate some of the side cracks along all or part of their lengths, building small lateral ridges analogous to formation of Class 1 or 2, but becoming part of an interbraided complex characteristic of Class 3. (d) If the weight of ridge complex warps the crust enough that part of the surface is below the water line, liquid may seep through the porous ridges and flood the margins, modifying and coloring the surface, as observed on Europa.

active at different times and possibly only along part of their length (Fig. 6c), perhaps reflecting changes in the stress field. This scenario provides a mechanism for development of the class 3 ridge structures, with their multiple ridge sets and braided, intertwined sequences of ridge formation.

Once the surface of the original ice crust is pushed down by the weight of the ridge to the level of the water line (independent of the class of the ridge structure), liquid water might spread over the surface (Fig. 6b). The ridges might act as levees to prevent lateral spreading of water. However, being built of crushed ice, the ridges are more likely to be porous. In that case, the liquid water could spread laterally through the base of the ridge and then flow across the surface beyond the ridges. This process might explain the emplacement of the reddish material that lines the outsides of the ridges, giving rise to the appearance of “triple-bands” at Voyager-like resolution. The darker, reddish coloring is probably due to impurities carried in the liquid water, perhaps silicates or organic material (Geissler 1998b), along with salts detected in the infrared (McCord *et al.* 1998). The relative lack of such darkening and coloration in the ridge material may be due to purification of the water as it froze in the cracks during our diurnal scenario.

Thus, a process of ridge formation based on diurnal working of cracks seems capable of explaining most of the defining characteristics of linear ridge structures on Europa.

V. GLOBAL DISTRIBUTION AND ORIENTATION OF TECTONIC FEATURES

A. Nonsynchronous Rotation

The discussion above considers how diurnal tides can activate and modify existing cracks to produce the kinds of extensive ridges associated with those presumably tectonic features. Next we consider how such cracks, including global-scale lineaments and pull-apart features, may have

formed initially. We investigate two sources of the required stress: diurnal tides (short period and low amplitude) and the tidal stress due to nonsynchronous rotation (longer period, higher amplitude).

In Section I we noted that the torque exerted by Jupiter on the dissipative lag components of the diurnal tide can yield nonsynchronous rotation, as discussed by Greenberg and Weidenschilling (1984). Moreover, the diurnal dissipation provides the heat source that may well be capable of maintaining the liquid water ocean central to our physical model above, and also of preventing the frozen-in global gravitational asymmetry that would be necessary to maintain synchronous rotation. Therefore, nonsynchronous rotation is a plausible past and current condition.

Comparing the positions relative to the terminator or the limb of features of Europa, as imaged by Voyager and by Galileo, Hoppa *et al.* (1997) placed constraints on the period of rotation (infinite for synchronous rotation) relative to the direction of Jupiter, finding it to be $>12,000$ yr. This long period is consistent with Earth-based photometric observations of the full disk of Europa, which showed hemispherical differences that have remained unchanged over decades, even if the leading hemisphere is not continually repainted by impacts or radiation. On the other hand, crater statistics on Europa do not show any detectable leading/trailing hemispheric asymmetry, which would be expected for synchronous rotation, suggesting that the rotation period is considerably less than the cratering age of the surface. Thus, the rotation period relative to Jupiter's direction is between $\sim 10^4$ yr and the crater age of the surface, where the latter might be as short as a few million years or as long as a few billion years, depending on estimates of the impact flux (Chapman *et al.* 1997).

B. Tidal Stress

1. *Tidal stress due to nonsynchronous rotation.* The tidal variation due to nonsynchronous rotation is about 30 times ($1/(7e)$) as large as the diurnal component. As the tidal bulge is reoriented relative to Europa's surface, stress accumulates. If the surface were in a relaxed state with a primary-component tidal bulge, and then nonsynchronous rotation reoriented the bulge by an angle of 1° , the surface stress field shown in Fig. 7 would accumulate. This stress is based on a model of an equilibrium configuration for a thin, uniform, elastic shell (similar to that assumed by Helfenstein and Parmentier 1983, based on a theory by Vening-Meinisz 1947 and Melosh 1980). Here we have assumed values of $\mu = 9.2 \times 10^9$ Pa for the shear modulus and $\nu = 0.33$ for the Poisson ratio (from Turcotte and Schubert 1982). The magnitude of the stress field is proportional to $\mu(1 + \nu)/(5 + \nu)$.

The pattern in Fig. 7 shows strong north-south tension centered at longitudes 45° and 225° and symmetrical com-

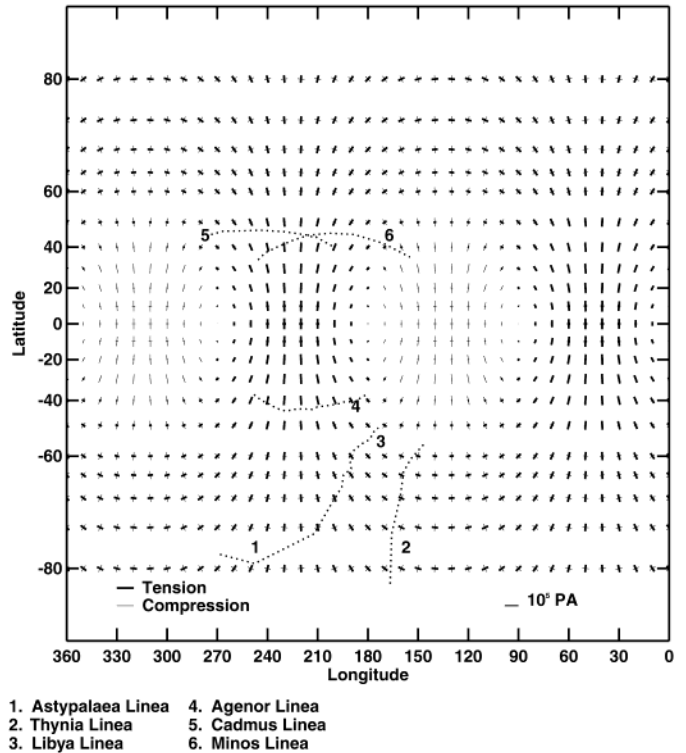


FIG. 7. Map of stress induced in a thin elastic shell due to a 1° rotation of a tidal bulge of the magnitude of Europa's primary tidal component. Crossed lines indicate the orientation and magnitude of the principal components, with bold lines indicating tension and fine lines indicating compression. Note scale bar for magnitude of the stress. Locations of several major European lineaments are indicated by dotted lines.

pression at 135° and 315° . The magnitude of the tension is comparable to the plausible tensile strength of the ice, and tension is the most likely mode of failure. Even at high latitudes, where there is substantial differential between principal stresses, the failure mode would not be shear (contrary to the results of Helfenstein and Parmentier 1985), because the principal stresses are nearly equal and opposite; if failure occurred, it would be tensile, according to consideration of the relationship between Mohr's circle and the failure envelope (Suppe 1985).

For any very small angle of rotation, the pattern is similar, with amplitudes approximately proportional to the angle and with symmetry offset from the cardinal longitudes (0° , 90° , 180° , 270°) by 45° . For example, the tension zones are centered at 45° west of the sub- and anti-Jupiter longitudes, similar to Fig. 7. More precisely, however, the pattern is actually shifted eastward from that orientation by a distance equal to half the rotation angle. Thus, if strain could accumulate over rotation by 30° (an example that would be possible only if the material were sufficiently elastic and strong), the stress patterns would be similar except shifted eastward by 15° , such that maximum tension

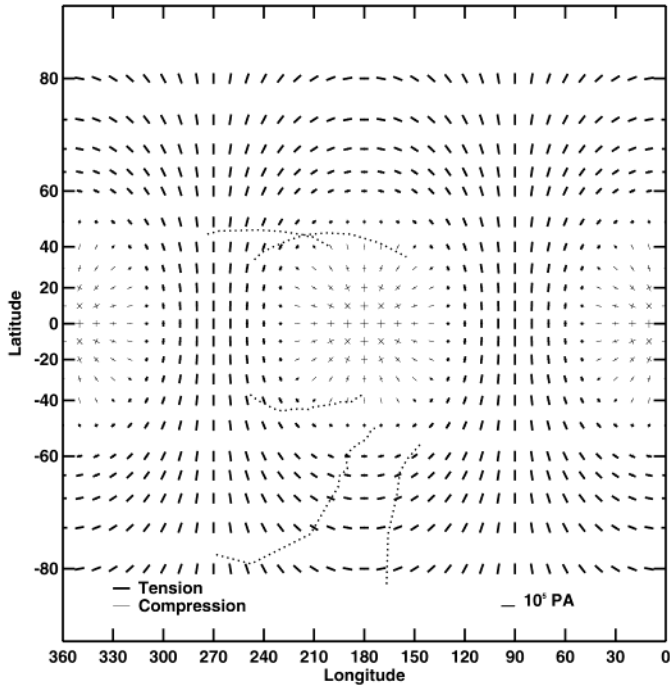


FIG. 8. Map of stress at apocenter, relative to the average tidal figure of Europa.

would be 30° west of the sub- and anti-Jupiter longitudes. (The displacement of the pattern by half of the rotation angle is a familiar consequence of taking the difference between sinusoidal functions offset in phase.)

2. *Tidal stress due to diurnal variations.* Diurnal variations are periodic over the 3.5 days of the orbital period. Figure 8 shows the tidal stress at apocenter relative to the average figure of Europa (i.e., the primary tidal figure without the diurnal components). Here with the distance from Jupiter at a maximum, the amplitude of the tidal bulge is a minimum, giving isotropic compression at the sub- and anti-Jupiter points and tension along the belt 90° from those points. The stress map at pericenter would be identical to Fig. 8, except that the signs of the principal components are reversed (e.g., tension becomes compression).

Because ice is most prone to failure in tension, we are especially interested in locations and conditions of maximum tension. The stress pattern represented by Fig. 8, like the pattern due to nonsynchronous rotation, has equatorial regions of north–south tension, although centered at quite different longitudes. Moreover, the tension extends across the poles, contrasting with the nonsynchronous case where tension near the poles is accompanied by comparable orthogonal compression yielding shear stress. In both cases (Figs. 7 and 8), the vectors of maximum tension form ellipses encircling regions that are under compression on the

equator: 0 and 180° for the diurnal stress, 135° and 315° for nonsynchronous stress.

It is important to remember that the diurnal tide is not simply due to the changing distance from Jupiter, but also to the changing direction of Jupiter (as shown in Fig. 1). Thus, after apocenter, the diurnal stress does not pass through zero. Instead, $1/8$ of an orbit after apocenter it forms the pattern shown in Fig. 9, and $1/4$ of an orbit after apocenter it forms the pattern shown in Fig. 10. In this sequence, we see the amplitude of the maximum tension along the equator increase (mostly in the $1/8$ orbit after apocenter) and the location of maximum tension and compression moves eastward. At $1/4$ orbit after apocenter, the pattern is identical to that for nonsynchronous rotation, because it represents a tidal bulge that is offset in direction by the small angle $2e$ radians (about 1°) from the average tide but with average tidal amplitude. The stress $1/2$ orbit later ($1/4$ orbit after pericenter) would be the same as Fig. 10, except with the signs of all stresses reversed.

C. Low Resolution Patterns from Voyager

Helfenstein and Parmentier (1985) identified sets of large-scale linear features on Europa that seemed to be consistent with orientations perpendicular to the maximum tension direction for a small extent of nonsynchronous rotation, providing a reasonable model for the formation of these lineaments because ice does fail most readily under

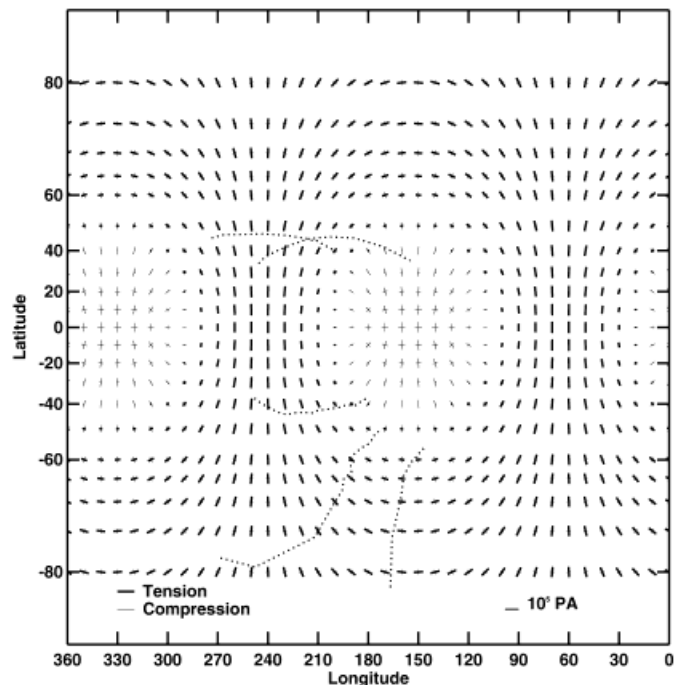


FIG. 9. Map of stress $1/8$ orbit after apocenter, relative to the average tidal figure of Europa.

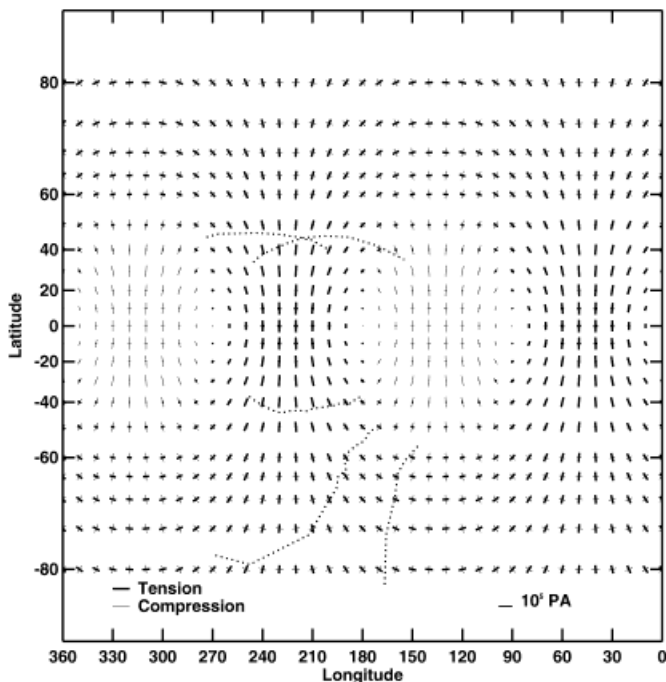


FIG. 10. Map of stress 1/4 orbit after apocenter, relative to the average tidal figure of Europa.

tension. An implication of that result would be that since cracking occurred there has been very little nonsynchronous rotation. Moreover, it would follow that if the rate of nonsynchronous rotation is currently in the low end of the range described in Section V.A, these cracks must be quite recent.

McEwen (1986) reported that most of the global scale lineaments fit the tension pattern for a small amount of nonsynchronous rotation (like Fig. 7) if that pattern were shifted eastward by 25°. In other words, the pattern indicates that after crack formation, Europa rotated another 25°. That result raises the question of why cracking responded to rotation only during one short interval, but not before or after. McEwen addressed that point by suggesting that the visible cracks were formed during several tens of degrees of nonsynchronous rotation, continually relieving stress accumulated over short intervals during that time, such that the average orientations fit the pattern from 25° of rotation ago.

Indeed, individual features do not all fit the nonsynchronous stress patterns of that particular epoch. For example, the orientation of Libya Linea is nearly perpendicular to maximum tension in the current nonsynchronous stress pattern as shown in Fig. 7. Thus, it fits recent nonsynchronous stress better than it would have fit in the past (i.e., better than if its position were further to the west when the crack first formed). Similarly, the orientation of the gray band Thynia Linea (Pappalardo and Sullivan 1996)

along most of its length fits more recent nonsynchronous stress better than it would have fit the nonsynchronous pattern in the past.

In order to explore the hypothesis that the observed cracks were formed due to stresses of nonsynchronous rotation, with such cracking occurring during tens of degrees of rotation, we next consider specific features and observational information on sequences of crack formation from cross-cutting relationships.

D. Time Variation Inferred from Imaging Data

1. *Cadmus–Minos intersection region.* Such a sequence has been discovered on Europa by Geissler *et al.* (1997, 1998a). Through multispectral image reconstruction and analysis in the general area of the intersection of the Cadmus and Minos Linea “triple bands” (longitude 10° to 60° west of the anti-Jupiter direction and latitude 25° to 65° north), Geissler *et al.* found a sequence of crack ages based on cross-cutting relations that correlate with evolution in color, which allow age sequencing based on color even where detailed cross-cutting information is lacking.

The youngest linear features in this region are narrow, apparently incipient cracks, less than a pixel (1.6 km) wide. These features are aligned with azimuth 15–25° south of east. Although not imaged at the high resolution that allowed us to define the three classes of linear features described in Section IV, these features are consistent with class 1 both in width and relative immaturity. Middle-aged features are the lineaments with dark reddish borders (triple bands in the terminology based on Voyager data), such as Cadmus and Minos Linea themselves. In terms of the model developed in Section IV, these bands are probably of class 2 or 3, where sufficient ridge material has been emplaced to allow downwarping and lateral flooding by reddish liquid. Lineaments of this type in this region trend generally east–west. Within this group of features, color reconstructions reveal a cross-cutting relationship between Cadmus and Minos Linea, with the younger Cadmus trending about 15° south of east and the older Minos trending about 15° north of east in the neighborhood of the intersection (as shown in Figs. 7–10). The oldest lineaments are much brighter than the triple bands and intermediate in color between the triple bands and the background icy plains, apparently a result of the aging process as discussed by Geissler *et al.* These oldest features trend generally toward 30° north of east.

This changing orientation of lineaments points to a clockwise rotation of the stress direction with time in this area. This sense of the rotation is consistent with migration due to nonsynchronous rotation of this region across a stress field. For example, if this region has moved from a location 50° west of its current longitude (relative to the direction of Jupiter), it moves across the instantaneous

(i.e., few degrees of rotation) nonsynchronous stress field as given by Fig. 7. Inspection of that field shows that the local direction of tension would indeed rotate systematically in the clockwise direction (it would be counterclockwise in the southern hemisphere).

Consider whether this rotation of the stress field for stresses due to nonsynchronous rotation (Fig. 7) is consistent with the observed orientations in this region. The orientation of the oldest lineaments in this region (azimuth 30° N of E) is consistent with the direction of tension in the nonsynchronous stress field (Fig. 7) at a location backward in rotation by about 40° (to a longitude that far to the west of the current position relative to Jupiter). Slightly to the west of the current position, the tension is maximum in the north–south direction, consistent with the generally east–west orientation of the middle-aged lineaments. However, this scenario fails to explain the orientation of the most recent cracks (and even Cadmus Linea), whose orientation would not be produced unless Europa were to continue to rotate somewhat further ahead from its current position.

This dilemma would be resolved if the stress pattern were shifted further west by 10° or more. Building up more than a few degrees of nonsynchronous stress would have exactly the opposite effect (shifting the pattern eastward), so it does not provide a solution, nor does diurnal stress alone. The stress pattern near apocenter would resolve the problem, but the magnitude of stress is greater three-quarters of an orbit earlier. Instead, consider a combination of the two sources of stress. As nonsynchronous stress builds up over >30 yr (likely much more) per degree, the surface also undergoes periodic diurnal stress. There is a gradual, monotonic increase in the strength of the nonsynchronous stress field, with the pattern shown in Fig. 7; the daily oscillations are superimposed upon it. Eventually, one day, the maximum diurnal stress added on top of the building nonsynchronous stress will exceed the strength of the surface material and cracking occurs.

To explore this scenario, we consider the combined diurnal and nonsynchronous stress fields. We are constrained to nonsynchronous stress corresponding to no more than about 1° of rotation; otherwise, the nonsynchronous stress will dominate and not give the needed shift of the pattern to the west. One degree of nonsynchronous rotation gives stress comparable in magnitude to the diurnal. At $1/4$ orbit before apocenter, the diurnal stress nearly exactly cancels out the nonsynchronous (this result follows from the discussion in Section V.B as well as by direct computation). At apocenter, the combined stress field gives substantial north–south tension ($>10^5$ Pa) and with a pattern such that the maximum tension is at 65° and 245° (instead of at 45° and 225° as in Fig. 7) giving the necessary westward shift. However, the maximum tension is still not reached at this point in the orbit.

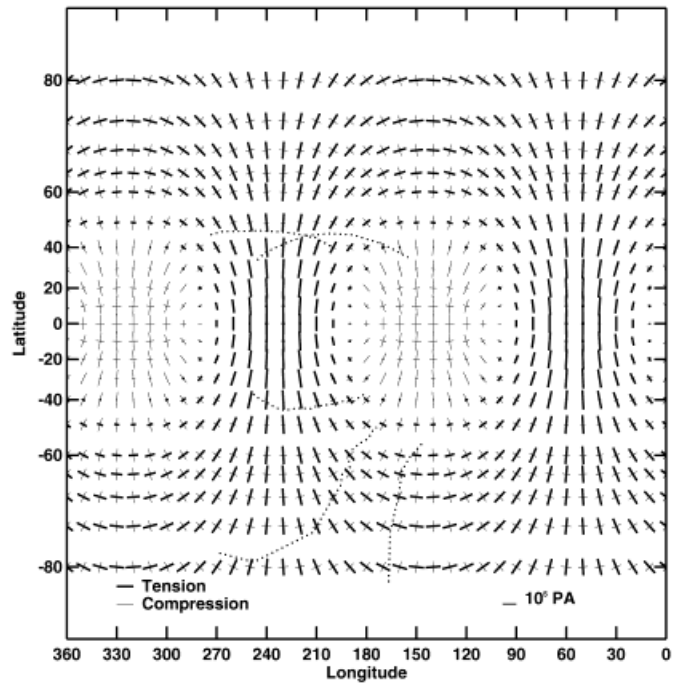


FIG. 11. Map of stress $1/8$ orbit after apocenter, added to the stress accumulated over 1° of nonsynchronous rotation. This pattern best fits (albeit imperfectly) the sequence of crack formation in the Cadmus/Minos intersection region.

The maximum in the region of interest is reached $1/8$ orbit after apocenter (shown in Fig. 11) and remains at about that level for the next $1/8$ of the orbit. Here we find tension $>1.5 \times 10^5$ Pa and a westward shift of the pattern relative to pure nonsynchronous rotation (Fig. 7) of about 10° . This stress magnitude is close to a plausible value of the tensile strength of the ice crust, based on estimates of the strength of sea ice (as low as 3×10^5 Pa according to Mellor 1986) and on scaling to the thicker crust of Europa which would reduce strength further. The shift of the stress pattern to the west is more consistent with a model in which the Cadmus/Minos intersection region has moved across the stress field from west to east.

This model has cracks forming in response to the maximum tension during diurnal tidal variations, at times when the combined diurnal and nonsynchronous stress exceeds the strength of the crust. In the region under consideration, the cracks formed orthogonal to the tension. According to the model of crack evolution discussed in Sections III and IV, after cracks form the diurnal tides can produce ridges, first of class 1, then of class 2 or 3, and eventually aging photometrically as well. As nonsynchronous rotation carries the region to a place where the stress field is sufficiently differently oriented, new sets of cracks form. Accordingly, the orientations and relative ages of cracks in the Cadmus/Minos intersection region fit the following

sequence of initial cracking relative to the rotational orientation:

1. The oldest cracks fit the pattern if they were formed at a time 60° backward in rotation, which might have been as recent as 2000 yr ago given our constraints on the rotation rate, but in any case long enough ago to allow the photometric aging.

2. Similarly, by inspection of Fig. 11, we find Minos formed about 40° ago.

3. Cadmus appears to have formed relatively recently ($<10^\circ$ ago) because in its current position it fits the stress field in Fig. 11 quite well. For Cadmus, as well as Minos, there has been adequate time since initial cracking for ridges to grow to class 2 or 3 structures. Assuming the model of ridge formation developed in Section III, such mature structures would require at least $\sim 10^5$ yr to develop, which implies a nonsynchronous rotation period of at least 3×10^6 yr.

4. The freshest cracks in this region, which run even more nearly north–south than Cadmus in this region, would not have formed until Europa reached its current orientation. At an earlier time, the tension would have been less nearly perpendicular to the direction of these lineaments. Even now the fit is not as good as it would have been if we could have found a way to shift the stress pattern even further west than in Fig. 11.

2. *Astypalaea Linea.* Information about change over time is also provided by observations of displacements at specific sites. The feature Astypalaea Linea (mapped on Figs. 7–11) runs nearly southward from about (60° S, 190° W), missing the south pole by about 10° , so as to run to the west and a few degrees northward. Tufts (1996) has shown that this feature has undergone right-lateral shear displacement of about 35 km. The orientation of this crack (along all its length) relative to the nonsynchronous stress pattern (Fig. 7) is at approximately a 45° angle relative to the principal axes of stress, such that the corresponding shear stress is consistent with the observed right lateral displacement. However, the principal stresses are of nearly equal and opposite signs, which is inconsistent with initial failure in the shear mode. More likely, initial cracking was due to tensile failure. The dominant tensile stress in this region is the diurnal stress near apocenter (Fig. 8). That stress fit the orientation of this crack quite well about 20° of rotation in the past, or fairly recently if the diurnal stress was superimposed on a small amount of nonsynchronous stress (see Fig. 11).

Once the crack formed, subsequent shear displacement occurred. The displacement may have been driven by the strong shear due to nonsynchronous stress (Fig. 7), but that tidal strain cannot explain the large shear distance of 35 km. Such large displacement can be explained by invoking cumulative effects of the diurnal tide, but by a mecha-

nism different from the ratcheting open of cracks that was described in Section III. Consider the diurnal stress in the region of Astypalaea Linea produced during each quadrant of every orbit. Around apocenter (Fig. 8) the crack is pulled open; $1/4$ orbit later (Fig. 9) the displacement is a right lateral shear. Next, the crack closes (Fig. 8 with reversed signs). Finally, the stress tries to shear in the left lateral sense, but shear is resisted by the fact that the crack has just clamped shut. In effect, by repeating this process during each orbital period, the crack “walks” in the right lateral direction. With plausible displacement of roughly a meter per orbit (the same scale of diurnal displacement discussed in Section III), the 35-km walk would require only a few thousand years. With less than ideal efficiency, the process would take longer, but migration is still possible in remarkably short times.

3. *Thynia Linea.* For the lineament Thynia Linea, just east of Astypalaea Linea, a similarly challenging displacement is observed, in this case by 25 km in the sense of crack opening (Pappalardo and Sullivan 1996). While Pappalardo and Sullivan noted that the orientation is perpendicular to the direction of tensile stress for nonsynchronous rotation, the agreement is really not very good and would have been even worse in the past. At least as good a fit is provided with the addition of the diurnal tension (Fig. 8) in this region, which would have been perpendicular to the crack orientation about 30° of rotation in the past, or more recently by diurnal tension superimposed on a small amount of nonsynchronous tension (Fig. 11).

4. *Libya Linea.* The orientation of Libya Linea, running northeastward from Astypalaea Linea, suggests formation about 20° of rotation in the past, according to inspection of Fig. 11. Moreover, there is some stratigraphic evidence of a time sequence of lineaments in the region where Libya meets Astypalaea (Tufts 1997). There may have been a counterclockwise formation sequence, in the sense that more recent features are oriented counterclockwise relative to older features. Although identification of this sequence is much more tentative than the clockwise sequence in the northern hemisphere at the Cadmus/Minos intersection, it suggests a similar cause. Migration of the region from west to east across the stress field shown in Fig. 11 would give the counterclockwise rotation of the local stress field, just as such migration gave clockwise rotation in the northern hemisphere.

5. *Agenor Linea.* Agenor (mapped on Figs. 7–11) appears to be a southern hemisphere analog to Cadmus and Minos, at the same distance from the equator. To be consistent with the symmetry implicit in our global interpretation, it should fit the same model of formation. Based on its longitudinal position, between that of Cadmus and Minos, our model suggests that it formed at a time when

Europa was 20° further back in its rotation than it is today. The morphology of Agenor has not yet been studied at resolution comparable to Cadmus and Minos, but imagery from the upcoming Galileo Europa Mission (GEM) should show whether it has similar characteristics, such as mature ridge structure. Photometric studies of Agenor (Geissler *et al.* 1998b) indicate that whenever the lineament was formed, it remains an active, developing feature, with possible recent frost deposits suggesting on-going working of the crack system.

VI. DISCUSSION

For the features considered above, we are led to a model in which diurnal tension provides the trigger for cracking, but it occurs after nonsynchronous rotation has built up a background stress, which allows the daily stress to exceed the critical strength level.

That conclusion is significantly different from previous interpretations. For example, consider the global lineaments that drove McEwen's (1986) model. His fitting was driven largely by the family of features roughly parallel to Minos Linea, which fit the tension orientations for nonsynchronous rotation at a time 25° of rotation ago. However, the sequence of cracking in the region near the Cadmus/Minos intersection forced us to adopt instead the model in which combined nonsynchronous and diurnal stresses created Minos (and presumably its parallel family of cracks) about 40° of rotation ago. Helfenstein and Parmentier (1983) compared crack patterns with the tension field during eccentric motion (or equivalently due to long-term orbital recession, which we rule out on the basis of the young age of the surface). Later (1985), they considered correlations with nonsynchronous stress. In both cases success was mixed. We have shown here that it is likely that both sources of stress were important, with cracking occurring when the building background of nonsynchronous stress adds to the maximum diurnal tension thereby exceeding the tensile strength of the crust.

In this study we have considered Europa's crust to be a uniform elastic sheet floating on a layer of liquid water. While this approximation is a useful, and perhaps the only, way to explore global stress patterns and effects, the real crust is much more complicated. In the lower portions of the crust, as the temperature approaches the melting point of water, the ice must be ductile on time scales that decrease with depth. For the diurnal elastic stress, we require that most of the crust be elastic over the diurnal time scale. For the component due to nonsynchronous rotation, we require that elastic stress develop over about 1° of rotation, which is about 100 yr for the fastest possible rotation consistent with orientations viewed by Voyager and Galileo, or about 10^4 yr for the fastest rotation consistent with the apparent age of Cadmus Linea (as discussed above).

Whether the bulk of the crust is elastic over 10^4 yr is problematic. For our model, it is not sufficient for only the upper portion of the crust to be elastic; the crust must stretch and crack through to liquid water.

A related concern is the role of lithostatic pressure. At depths greater than 100 m, the weight of the ice above creates hydrostatic pressure comparable to the elastic stress that we have invoked to crack the ice. If such pre-stressing effectively strengthens the ice at depth, it might inhibit cracking through to a liquid layer.

On the other hand, even with the hydrostatic pressure, it may be possible for the extension to yield deep cracks. The cracking process is initiated by very rapid global strain over a few hours and the crack propagation is a rapid and dynamic process, which may not be constrained by equilibrium considerations. Moreover, as stress is relieved by cracking near the surface, it is concentrated at the bottom of the crack, driving material failure still deeper. Similarly, during propagation of linear cracks along the surface, stress is concentrated at the ends of the cracks, possibly far exceeding the level of stress computed for the intact ice shell. In addition, while hydrostatic preloading can limit horizontal tension at depth, the strain imposed by tides produces a differential between the vertical lithostatic compression and the horizontal component, such that the crack may continue to propagate downward, although not necessarily directly vertically. Finally, it is possible that cracks that initiate in the elastic upper portion of the crust are able to propagate further downward during subsequent diurnal working, as trapped debris ratchet the cracks open further. Our model of crack formation and evolution requires that some such processes do allow cracks to propagate completely through the crust.

Another assumption of our model is that the crust is uniform over the entire globe. Deviations from such uniformity must, in fact, produce regional heterogeneity and deviations from the global stress distributions that we have computed here. Cracking itself modifies the crust and the global stress. Such effects mean that we cannot expect to be able to fit all lineaments to this simple theoretical model. Even the most prominent, global-scale features (such as the ones we have highlighted in this paper) can at best be approximated by this model.

In this paper we have considered large-scale lineaments for which we have some geological evidence for evolution with time and explored whether they can be correlated with global-scale sources of stress. A complete, systematic explanation of all cracking may be impossible for other reasons in addition to regional variations. For example, the complex, multiply overlying linear features on Europa suggest a long-term evolution reflecting great changes in the sources of stress themselves. They may represent the effects of nonsynchronous rotation over several periods

or of polar wandering, such that orderly monotonic time sequences would be obscured.

Indeed, there are major linear features that do not directly fit our global model. Most prominent are the globe-encircling lineaments that cross the equator at oblique orientations, generally near longitudes 90° and 270° . In all of the stress fields we have considered, tension at the equator is predominantly oriented north–south, a gross mismatch with the observed features. One such feature appears to be an extension of Asterius Linea along a great circle. Perhaps the large, obliquely equator-crossing lineaments were formed by a lengthening and joining of cracks like Minos with their symmetrical counterparts on the opposite side of the globe, with the propagation rapidly enhanced by the readjustment of the stress field as the cracking continues.

A type of large-scale lineament that we have not addressed here so far is the arcuate, or cycloidal, ridge. These common features are chains of arcuate segments, as seen in plan view, joined at cusps so as to give a cycloidal pattern. Galileo imaging on orbit G7 has included moderate resolution (510 m/pixel) coverage of at least one arcuate ridge, revealing a class 1 (double ridge) structure, which implies working along a crack in the crust, according to the model introduced here. It has been speculated that the arcuate lineaments are the result of thrust faulting (e.g., Helfenstein and Parmentier 1983). Nolan and Greenberg (1987) showed that horizontal compression could produce arcuate structures during incipient downwarping. Downwarping of part of a spherical shell is most efficiently accommodated by bending along an arc. Based on a model of energetic efficiency, Greenberg and Nolan found that the scale of the arcs on European ridges was consistent with a crustal thickness of several kilometers and horizontal displacement of a few hundred meters (proportional to the square root of the thickness). Thus, these features might represent the sites of compression needed on a global scale to accommodate the substantial extension revealed by many other features.

The essence of that explanation for the arcuate shapes is that, when the radius of curvature of a spherical cap is effectively reduced, its edges tend to fold into arcuate creases. This effect could be due to compression and downwarping as described above. However, on-going changes in regional radius-of-curvature would also occur as portions of the surface move across the tidal bulge during nonsynchronous rotation or simply due to diurnal tidal variations. We note that most of the known arcuate ridges lie along circles surrounding the anti-Jupiter point, perhaps caused by the reduction in radius of curvature in that region at pericenter. Such a process could provide an explanation for the arcuate structures, a model that deserves further study as we obtain data that allow us to understand the global distribution and ages of the cycloidal ridges. More

generally, the effects of bending stresses in the crust, which have not been addressed in this paper, need to be given careful consideration.

In the scenario developed here, we have not considered the effects of long-term orbital and rotational changes. Changes in the rotation rate, for example due to spin-down from the primordial rate, would induce significant stresses. Changes in the orbit, including plausible changes in distance from Jupiter and in orbital eccentricity (e.g., Greenberg 1989, Showman and Malhotra 1997) also likely affected stresses, as well as the thermal history and other geophysical processes, in important ways. Changes in the radius of Europa during its geophysical evolution were probably another source of surface stress. Here we have assumed that Europa's surface is so young that all those effects have long since been erased. If cratering ages are revised to suggest an older surface, the entire scenario developed here would need to be reconsidered. Another important issue may be polar wander (e.g., Ojakangas and Stevenson 1989b), which could cause the stress field to vary relative to the geographical features on Europa's surface.

We have shown that diurnal tides, as well as nonsynchronous rotation, can create significant stress fields on Europa's surface. Because ice is plastic over long periods, and because we have found that any nonsynchronous rotation is slow, nonsynchronous stresses cannot build up throughout the crust over more than a few degrees of rotation, and they are thus comparable to the stresses of the smaller but much more frequent diurnal tidal variation. Patterns and time sequences of apparent cracking on Europa include features that correlate with both sources of stress combined and appear to represent cracking that occurred over the past several tens of degrees of nonsynchronous rotation.

Once cracking is initiated, diurnal tides could work cracks so that they open and close daily. Although the daily effect is small, over tens of thousands of years ridges can be built along the cracks that fit the size and morphologies of observed structures. Our model of the origin, growth, and maturation of these features fits the time sequence of features in the Cadmus and Minos Linea region (Geissler *et al.* 1997, 1998a) that is consistent with the diurnal tensile-stress field, as it evolves under nonsynchronous rotation, and it seems consistent with other major lineaments as well.

The success of this model at fitting large-scale lineaments in various regions provides evidence for the presence of a liquid-water layer, as well as for nonsynchronous rotation. If the mantle were solid or viscous, instead of liquid water, the diurnal tidal amplitude would be much smaller than the 15 m assumed in our calculations, while the nonsynchronous component could still have the full kilometer-scale amplitude. In that case, the combination of tidal stress components required to fit the large-scale crack patterns

would not be attained. The water mantle is required in order to have a significant amplitude to the diurnal component.

ACKNOWLEDGMENTS

We thank the technical staff of the Galileo project for making this project possible through all phases of development and operations. The members of the imaging team, led by Mike Belton, and their associates provided stimulating scientific discussion and interaction, which was essential for framing the analysis discussed here. Greg Ojakangas provided a careful review of the manuscript. Theoretical aspects of this work were supported by NASA's Planetary Geology and Geophysics program.

REFERENCES

- Belton, M. J. S., and 33 colleagues 1996. Galileo's first images of Jupiter and the Galilean satellites. *Science* **274**, 377–384.
- Carr, M. H., and 21 colleagues 1998. New evidence for a global ocean on Europa. *Nature* **391**, 363–365.
- Cassen, P. M., S. J. Peale, and R. T. Reynolds 1982. Structure and thermal evolution of the Galilean satellites. In *Satellites of Jupiter* (D. Morrison, Ed.), pp. 93–128. University of Arizona Press, Tucson.
- Chapman, C. R., and 17 colleagues 1997. Populations of small craters on Europa, Ganymede and Callisto. *Lunar Planet. Sci.* **XXVIII**, 235–236.
- Geissler, P., and 13 colleagues 1997. Galileo multispectral imaging of Europa: Evidence for nonsynchronous rotation. *Lunar Planet. Sci.* **XXVIII**, 401–402.
- Geissler, P. E., R. Greenberg, G. Hoppa, P. Helfenstein, A. McEwen, R. Pappalardo, R. Tufts, M. Ockert-Bell, R. Sullivan, R. Greeley, M. J. S. Belton, T. Denk, B. Clark, J. Burns, J. Veverka, and the Galileo Imaging Team 1998a. Evidence for non-synchronous rotation of Europa. *Nature* **391**, 368–370.
- Geissler, P. E., R. Greenberg, G. Hoppa, A. McEwen, R. Tufts, C. Phillips, B. E. Clark, M. Ockert-Bell, P. Helfenstein, J. Burns, J. Veverka, R. Sullivan, R. Greeley, R. T. Pappalardo, J. W. Head III, M. J. S. Belton, and T. Denk 1998b. Evolution of lineaments on Europa: Clues from Galileo multispectral imaging observations. *Icarus* **135**, 107–126.
- Greeley, R., R. Sullivan, J. Klemaszewski, K. Homan, J. W. Head III, R. T. Pappalardo, J. Veverka, B. E. Clark, T. V. Johnson, K. P. Klaasen, M. Belton, J. Moore, E. Asphaug, M. H. Carr, G. Neukum, T. Denk, C. R. Chapman, C. B. Pilcher, P. E. Geissler, R. Greenberg, and R. Tufts 1998. Europa: Initial Galileo geological observations. *Icarus* **135**, 4–24.
- Greenberg, R. 1989. Time-varying orbits and tidal heating of the Galilean satellites. In *Time-Variable Phenomena in the Jovian System* (M. Belton, R. West, and R. Rahe, Eds.). NASA Special Publication no. 494.
- Greenberg, R., and S. J. Weidenschilling 1984. How fast do Galilean satellites spin? *Icarus* **58**, 186–196.
- Helfenstein, P., and E. M. Parmentier 1983. Patterns of fracture and tidal stresses on Europa. *Icarus* **53**, 415–430.
- Helfenstein, P., and E. M. Parmentier 1985. Patterns of fracture and tidal stresses due to nonsynchronous rotation: Implications for fracturing on Europa. *Icarus* **61**, 175–184.
- Hoppa, G. V., R. Greenberg, P. Geissler, J. Plassmann, B. R. Tufts, and Galileo Imaging Team. 1997. Rotation of Europa: Constraints from terminator positions. *Lunar Planet. Sci.* **XXVIII**, 597–598.
- Jeffreys, H. 1961. The effect of tidal friction on eccentricity and inclination. *Mon. Not. Roy. Astron. Soc.* **122**, 339–343.
- Lucchita, B. L., and L. A. Soderblom 1982. The geology of Europa. In *Satellites of Jupiter* (D. Morrison, Ed.), pp. 521–555. University of Arizona Press, Tucson.
- McCord, T. B., G. B. Hansen, F. P. Fanale, R. W. Carlson, D. L. Matson, T. V. Johnson, W. D. Smythe, J. K. Crowley, P. D. Martin, A. Ocamo, C. A. Hibbits, J. C. Granahan, and the NIMS Team 1998. Salts on Europa's surface detected by Galileo's near infrared mapping spectrometer. *Science* **280**, 1242–1245.
- McEwen, A. S. 1986. Tidal reorientation and the fracturing of Jupiter's moon Europa. *Nature* **321**, 49–51.
- Mellor, M. 1986. Mechanical behavior of sea ice. In *The Geophysics of Sea Ice* (N. Untersteiner, Ed.), pp. 165–282. Plenum Press, New York.
- Melosh, H. J. 1980. Tectonics patterns on a tidally distorted planet. *Icarus* **43**, 334–337.
- Morrison, D., D. P. Cruikshank, and J. A. Burns 1977. Introducing the satellites. In *Planetary Satellites* (J. A. Burns, Ed.), pp. 3–17. University of Arizona Press, Tucson.
- Nolan, M., and R. Greenberg 1987. Cycloidal ridges on Europa: Analogs to Earth's island arcs. *Bull. Am. Astron. Soc.* **19**, 860.
- Ojakangas, G. W., and D. J. Stevenson 1989a. Thermal state of an ice shell on Europa. *Icarus* **81**, 220–241.
- Ojakangas, G. W., and D. J. Stevenson 1989b. Polar wander of an ice shell on Europa. *Icarus* **81**, 242–270.
- Pappalardo, R. T., and M. D. Coon 1996. A sea-ice analog for the surface of Europa. *Lunar Planet. Sci.* **XXVII**, 997–998.
- Pappalardo, R. T., and R. J. Sullivan 1996. Evidence for separation across a gray band on Europa. *Icarus* **123**, 557–567.
- Parmerter, R. R., and M. D. Coon 1972. Model of pressure ridge formation in sea ice. *J. Geophys. Res.* **77**, 6565–6575.
- Peale, S. J. 1977. Rotational histories of the natural satellites. In *Planetary Satellites* (J. A. Burns, Ed), pp. 87–112. University of Arizona Press, Tucson.
- Peale, S. J., P. Cassen, and R. T. Reynolds 1979. Melting of Io by tidal dissipation. *Science* **203**, 892–894.
- Reynolds, R. T., S. W. Squyres, D. S. Colburn, and C. P. McKay 1983. On the habitability of Europa. *Icarus* **56**, 246–254.
- Ross, M., and G. Schubert 1987. Tidal heating in an internal ocean model of Europa. *Nature* **325**, 132–134.
- Schenk, P. M., and W. B. McKinnon 1989. Fault offsets and lateral crustal movement on Europa: Evidence for a mobile ice shell. *Icarus* **79**, 75–100.
- Showman, A. P., and R. Malhotra 1997. Tidal evolution into the Laplace resonance and the resurfacing of Ganymede. *Icarus* **127**, 93–111.
- Squyres, S. W., R. T. Reynolds, P. Cassen, and S. J. Peale 1983. Liquid water and active resurfacing on Europa. *Nature* **301**, 225–226.
- Suppe, J. 1985. *Principles of Structural Geology*. Prentice-Hall, Englewood Cliffs, NJ.
- Tufts, B. R. 1993. Photogeological analysis of european tectonic features. *Lunar Planet. Sci.* **XXIV**, 1445–1446.
- Tufts, B. R. 1996. A San Andreas-sized strike-slip fault on Europa. *Lunar Planet. Sci.* **XXVII**, 1343–1344.
- Tufts, B. R. 1998. *Lithospheric Displacement Features on Europa, and Their Interpretation*. Dissertation, Univ. of Arizona.
- Turcotte, D. L., and G. Schubert 1982. *Geodynamics*. Wiley, New York.
- Vening-Meinisz, F. A. 1947. *Shear Patterns of the Earth's Crust*. Trans. AGU 28, pp. 1–61.